Tree Physiology 38, 243–251
doi:10.1093/treephys/tpx138

Research paper

Functional relationships between wood structure and vulnerability to xylem cavitation in races of *Eucalyptus globulus* differing in wood density

Antonio José Barotto[1,2,5], Silvia Monteoliva[1,2], Javier Gyenge[2,3], Alejandro Martinez-Meier[4] and María Elena Fernandez[2,3]

[1]Instituto de Fisiología vegetal (INFIVE), Facultad de Ciencias Agrarias y Forestales, Universidad Nacional de La Plata, CC 31 (1900) La Plata, Argentina; [2]Consejo Nacional de Investigaciones Científicas y Técnicas (CONICET), Argentina; [3]INTA, EEA Balcarce-Oficina Tandil, CC 370 (7000) Tandil, Argentina; [4]INTA, EEA Bariloche. CC 277 (8400) Bariloche, Argentina; [5]Corresponding author (jbarotto@conicet.gov.ar)

Received April 19, 2017; accepted October 3, 2017; published online November 21, 2017; handling Editor Maurizio Mencuccini

Wood density can be considered as a measure of the internal wood structure, and it is usually used as a proxy measure of other mechanical and functional traits. *Eucalyptus* is one of the most important commercial forestry genera worldwide, but the relationship between wood density and vulnerability to cavitation in this genus has been little studied. The analysis is hampered by, among other things, its anatomical complexity, so it becomes necessary to address more complex techniques and analyses to elucidate the way in which the different anatomical elements are functionally integrated. In this study, vulnerability to cavitation in two races of *Eucalyptus globulus* Labill. with different wood density was evaluated through Path analysis, a multivariate method that allows evaluation of descriptive models of causal relationship between variables. A model relating anatomical variables with wood properties and functional parameters was proposed and tested. We found significant differences in wood basic density and vulnerability to cavitation between races. The main exogenous variables predicting vulnerability to cavitation were vessel hydraulic diameter and fibre wall fraction. Fibre wall fraction showed a direct impact on wood basic density and the slope of vulnerability curve, and an indirect and negative effect over the pressure imposing 50% of conductivity loss (P_{50}) through them. Hydraulic diameter showed a direct negative effect on P_{50}, but an indirect and positive influence over this variable through wood density on one hand, and through maximum hydraulic conductivity ($k_{s\ max}$) and slope on the other. Our results highlight the complexity of the relationship between xylem efficiency and safety in species with solitary vessels such as *Eucalyptus* spp., with no evident compromise at the intraspecific level.

Keywords: *Eucalyptus globulus*, path analysis, vulnerability to cavitation, wood anatomy, wood density, xylem hydraulic conductivity.

Introduction

Wood anatomy of the *Eucalyptus* genus has particular characteristics (solitary vessels, vasicentric tracheids and fibre-tracheids, among others) determining a singular functionality, which has not yet been extensively studied (Barotto et al. 2016), as well as a wide wood density range (InsideWood 2004–onwards). Wood density can be considered as a measure of the internal wood structure, representing the combination of the different cell types that compose it (Ziemińska et al. 2013). It is usually used as a proxy measure of other mechanical and functional traits since it is strongly correlated with a variety of functional process (Lachenbruch and McCulloh 2014). In particular, there is evidence indicating that—at the interspecific level—wood density is negatively correlated with xylem vulnerability to cavitation, in the sense that a greater resistance in this process (i.e., xylem reaching higher tension) is associated with higher wood density

(Hacke et al. 2001, Jacobsen et al. 2005). This correlation could be explained by the need for cell wall reinforcement on conductive elements (Hacke et al. 2001) and/or by the contribution that non-conductive elements (fibre matrix) make to maintain equilibrium during water transport under high tension (Jacobsen et al. 2005, 2007). These relationships have been found by analysing a broad set of species, but studies focused on the intraspecific level are scarce. If the functional adaptive role of wood density was as previously proposed, the same trends would be expected to be observed within species, when considering genotypes with differences in wood density. Studies relating wood micro-density within different growth ring portions and vulnerability to cavitation in *Pseudotsuga menziesii* (Dalla-Salda et al. 2011, 2014) and *Picea abies* (Rosner 2013) suggest that this relationship is also observed at the intraspecific level. However, the fact that these relations only emerge when considering specific portions of growth ring suggests that causal relationships among traits are far from being elucidated and extrapolated to other species, particularly to non-conifers. In this regard, to our knowledge, there is no background of studies that explore these relationships at the intraspecific level in angiosperms.

Eucalyptus globulus Labill. is one of the most important commercial forestry species worldwide (Drew et al. 2009), but its growth is significantly affected by water availability (Drew et al. 2008). Climate projections predict an increase in the extent and severity of drought periods over many regions of the Earth (Dai 2013), including areas of native and cultivated *Eucalyptus* forests. The analysis of wood structure and its relation with vulnerability to cavitation allows evaluation of how water transport varies within xylem as a function of water stress (Cochard et al. 2013). It directly affects the drought tolerance of different species and *Eucalyptus* in particular (Vander Willigen and Pammenter 1998) and, therefore, influences productivity (Sperry 1995, Hubbard et al. 2001) and survival (Maherali et al. 2004) under stress conditions.

The relationship between wood density and vulnerability to cavitation has been little studied in the *Eucalyptus* genus, where the presence of solitary vessels make unlikely the imbalance of forces proposed by Hacke et al. (2001), thus requiring specific hypotheses. In this regard, some studies (Vander Willigen and Pammenter 1998, Tesón et al. 2012, Barotto et al. 2016) have evaluated the cavitation resistance in *Eucalyptus* species with different wood density. The general trend at the interspecific level shows that low wood density species are more vulnerable to cavitation. Nevertheless, intraspecific analysis is hampered by the anatomical complexity of this genus. Therefore, it becomes necessary to address more complex techniques and analyses to elucidate the way in which the different anatomical elements are functionally integrated. Path analysis, a particular case of structural equation modelling, is a multivariate method that allows evaluation of the adjustment of theoretical causal models in which a set of dependency relationships between variables is proposed (Pérez et al. 2013). Path analysis is an extension of multiple regression (Norman and Streiner 2003) where not only is the direct contribution of independent variables over a dependent one verified, but also the interaction between predictor variables and their indirect effect (Pérez et al. 2013).

To contribute to the knowledge about the relationships between wood structure and function in the *Eucalyptus* genus, races of *E. globulus* with high and low stem wood density were analysed. The objectives of this study were: (i) to characterize in detail the morphometry of wood anatomical elements from *E. globulus* races with differences in stem wood density, (ii) to determine the vulnerability to cavitation of selected races, (iii) to establish relationships between anatomical traits and the wood properties derived from them and (iv) to propose and validate a model that explains how these characters and properties are related (directly and/or indirectly), determining the cavitation resistance in this species. Our general hypotheses about the relationships between variables were based on antecedents for the genus, considering that the same relationships would apply at the intraspecific level. In this regard, we expected that higher wood density genotypes would present greater resistance to cavitation, and no trade-off between xylem efficiency (maximum hydraulic conductivity) and xylem safety, through the significant influence of vessel size distribution on vulnerability to cavitation (i.e., xylem with a broader range of vessel sizes, including larger vessels, will be related to lower pressure imposing 50% of conductivity loss (P_{50}) as observed at the interspecific level by Barotto et al. 2016).

Materials and methods

Site and plant material

The plant material used in this study is part of a trial that belongs to the Genetic Improvement Programme of *E. globulus* (Labill.) from the Instituto Nacional de Tecnología Agropecuaria (INTA) of Argentina, in which 250 progenies belonging to 12 native races from Australia were planted in 1995 (Lopez et al. 2001). The field trial was located in Balcarce, Buenos Aires province, Argentina (37°45′S, 58°17′W, 97 m above sea level). The climate of this region is defined, according to Köppen climate classification, as oceanic. The mean annual temperature is 13.3 °C, and the mean annual precipitation is about 800 mm. The individuals were 20 years old when the sampling was carried out, and the selection was based on previous information on wood density estimation using Pilodyn over standing trees. The two races whose mean wood densities were located at the opposite extremes (upper and lower) of wood density range were selected (for detailed information about the trial see Table S1 available as Supplementary Data at *Tree Physiology* Online).

Sample collection and processing

Sample collection was carried out during the first days of February 2015, in the early morning (before 9 a.m.) during a

time period with high soil water availability, to minimize water stress. Six trees of every race were selected ($n = 6$), and two branches were extracted from each tree from the basal portion of the crown, taking care that they were of similar dimensions (3.1–5.7 mm in diameter), totalizing 24 branches. Branches were re-cut underwater and stored in black polyethylene bags, wrapped with wet rags to avoid drying.

In the lab, branches were re-cut again underwater to their final length. Barotto et al. (2016) demonstrated that branch lengths greater than 30 cm produce S-shaped curves in *Eucalyptus* spp., so this measure was taken as a minimum length. Branches were debarked and stored in distilled water with 1% sodium hypochlorite at 4 °C (Jinagool et al. 2015) to avoid the development of microbial activity until its use (no more than 2 weeks).

Vulnerability to cavitation curves

Vulnerability to cavitation (VC) curves were developed using a Scholander pressure chamber (model 10, BioControl, Buenos Aires, Argentina) with a cavitation chamber attached to it. The protocol followed was:

(i) perfusion during 15 min at 1 Bar pressure to remove any initial embolism;
(ii) maximum hydraulic conductivity measurement ($k_{s\ max}$) with the pipette method (Sperry et al. 1988);
(iii) constant pressure applied within the cavitation chamber for 2 min (from −0.5 to −6.5 MPa, every 1 MPa);
(iv) stabilization until constant k_s (no bubbles coming out from the branch extremes);
(v) k_s measurement.

Steps (i) and (ii) were performed only at the beginning of each curve, whereas steps (iii)–(v) were repeated for each point of every curve.

The percentage loss of hydraulic conductivity (PLC) was estimated from the k_s losses for every imposed pressure level in relation to the maximum k_s ($k_{s\ max}$) of each branch. Once the VC curve was completed, the cumulative density function (CDF) of Weibull distribution was fitted to it:

$$PLC/100 = 1 - \exp[-(T/b)^c]$$

where T is the tension (considered as equal in absolute value to the positive pressure applied in the cavitation chamber), b is the Weibull scale parameter and c is the Weibull shape parameter. Usual parameters like P_{50}, P_{12} and P_{88} (that is, pressure inducing 50%, 12% and 88% losses of hydraulic conductivity) and the slope between P_{12} and P_{88} of each VC curve (which denotes how fast conductivity is lost) were estimated from this model. P_{12} corresponds to air entry point (Sparks and Black 1999), and P_{88} is considered the point beyond which xylem becomes completely non-conductive (Domec and Gartner 2001).

Anatomical variables

Once VC curves were done, branches were adequately conditioned to obtain histological sections for anatomical measurements (24 branches, 12 for each race corresponding to six different individuals). Cross sections (20–25 μm thick) of the entire transversal branch section were obtained using a sliding microtome. Histological sections were not stained and were mounted in water. The following variables were measured in transverse sections: vessel density (VN, mm^{-2}), halo area (H, μm^2; this term is used to refer to the area occupied by all companion cells surrounding a solitary vessel, and it is composed of vasicentric tracheids (VT) and axial parenchyma, see Barotto et al. (2016) for a more detailed explanation of this trait), fibre wall thickness (FWT, μm), fibre wall fraction (WF, %) and rays per linear millimetre (Rn, no. mm^{-1}). In addition, macerations were prepared according to Franklin (1945): 1 cm-long segments were cut from each branch and soaked in a 1:1 glacial acetic acid: hydrogen peroxide solution. The following measurements were taken: fibre percentage (Fp, %), fibre-tracheid percentage (FTp, %), VT percentage (VTp, %), axial parenchyma percentage (APp, %), fibre length (Fl, μm), fibre-tracheid length (FTl, μm), VT length (VTl, μm) and vessel element length (Vl, μm).

Cross-sectional and maceration images were captured with a digital camera (Infinity1-2CB, Lumenera Corporation, Ottawa, Canada), mounted on a research microscope (CX31, Olympus, Tokyo, Japan), using a magnification of 4× (20–25 images to capture the entire branch transversal section) and 20× (20 images to cover two complete radial sections from pith to bark). Captured images were analysed using image analysis software (ImagePro Plus 6.0, Media Cybernetics, Carlsbad, CA, USA).

Wood basic density (WBD, g cm^{-3}) at branch level was determined as oven-dry mass per unit of fully saturated wood volume.

Vessel hydraulic diameter (Dh, μm) was estimated from vessel diameter (D, μm) measurements with the following equation:

$$Dh = \Sigma D^5/\Sigma D^4$$

Since previous studies (Barotto et al. 2016) demonstrated a meaningful relationship between vessel size distribution and VC at the interspecific level in this genus, vessel percentage in different diameter size classes was fitted with Weibull probability density function (PDF):

$$PDFV\ (x;\ b,\ c)\ =\ c/b\ (x/b)^{(c\ -\ 1)}\ \exp[-(x/b)]^c$$

where b and c are fitting constants (equivalent to those of Weibull CDF), and x is the vessel diameter class size. Parameters b and c describe the amplitude and shape (more or less symmetrical) of vessel distribution, respectively.

Statistical analyses

Statistical differences in wood density, anatomical and hydraulic traits between races ($\alpha = 5\%$) were tested with analysis of

variance (ANOVA) followed by a Fisher's LSD post-hoc analysis. Contingency tables were used to establish differences among races in vessel size distribution and vulnerability to cavitation curves. Relationships between pairs of variables at individual level were analysed using Pearson correlation analysis. These analyses were made with InfoStat statistical software (v. 2015, InfoStat group, FCA, Universidad Nacional de Córdoba, Córdoba, Argentina).

Model specification

Once we had statistical information about the differences in traits between races and how these traits correlated with each other, we started to develop a model, selecting first those variables that presented differences between races, and later we added those variables that showed significant correlations with others. By doing this, we tried to minimize the number of variables in order to achieve the simplest model able to reflect the major relationships among variables. We selected P_{50} as the primary indicator of resistance to cavitation since it is the most commonly used parameter for comparing sensitivity to this process.

The path analysis technique relies on path diagrams that allow the links among variables to be modelled easily. These are represented by rectangles, and each path is represented by a straight line with an arrow head, the direction of which indicates the direction of the relationship. Correlations among variables are represented by double-headed lines (Norman and Streiner 2003). Through these diagrams, it is possible to distinguish the associations between variables in terms of direct and indirect effects. The direct effect of one variable over another is estimated through path coefficients, which are similar to beta weights in a multiple regression. The magnitude of the indirect effect is the result of multiplying the path coefficients between two related variables.

There are two types of variables: exogenous and endogenous variables. Exogenous variables are those whose causes (predictors) are external to the model, and their function is to explain the other internal variables of the model. They have paths coming from them and none leading to them (correlations are not considered paths). Endogenous variables have their causes in one or more model variables. They have at least one path leading to them (Pérez et al. 2013).

With this in mind, we considered as exogenous variables the anatomical traits that do not depend on any other, with all the remaining being endogenous variables. We started by creating the exogenous variables and linking them with double-headed arrows. Then, we added the endogenous variables and connected them based on the magnitude and significance of the correlation analysis. In the arrangement of the variables and their interconnection, we tried to address the possible causal effects, based on bibliography and our expertise.

From this initial model, we started an iterative process where we first looked at the individual components of the model (regression weights of every path and their significance levels), trimming the paths that were non-significant (P-value $\geq$0.05). These were estimated by maximum likelihood method, which is not dependent on the scale of measurement. At the same time, we analysed the fit of the model as a whole with several goodness-of-fit tests (Table 1). There are two kinds: indices of absolute fit and indices of comparative fit (respect to another model). None of these tests alone provides all the information needed to evaluate the model so, usually, a set of them is used simultaneously. More details about the different indices can be found in Ullman (2013). Finally, once we had reached a model with only significant paths, we proceeded with model re-specification in order to improve it and get a better fit. For this purpose, we looked at the modification indices given by the software (SPSS AMOS 22.0.0, IBM Corp., Armonk, NY, USA).

Results

Wood anatomy

In agreement with the determination of stem wood density carried out with Pilodyn on standing trees, races differed significantly in branch WBD (Table 2). However, there were no differences in hydraulic diameter, vessel density (i.e., the number of vessels per unit area) or vessel element length, suggesting a similar hydraulic architecture at xylem tissue level. In this regard, the analysis of contingency tables for vessel size distribution showed no differences between races ($\chi^2 = 5.17$, $P = 0.52$). Added to this, the parameters describing the amplitude and shape of vessel distribution adjusted with Weibull PDF (b and c, respectively) did not vary between races.

Table 1. Goodness-of-fit tests and the statistical criterion used to evaluate the model fit (Ullman 2013).

Test	Abbreviation	Criterion
Absolute fit indices		
Chi-square	χ^2	Significance >0.05
Relative chi-square	χ^2/df	<2
Goodness-of-Fit Index	GFI	>0.9
Root Mean Square Error of Approximation	RMSEA	<0.06
Standardized Root Mean Square Residual	SRMR	<0.08
Comparative fit indices		
Normed Fit Index	NFI	>0.95
Tucker-Lewis Index	TLI	>0.95
Comparative Fit Index	CFI	>0.95

Table 2. Mean ± standard deviation of anatomical variables measured in two races of *Eucalyptus globulus* with high and low stem wood density respectively (12 branches of each race corresponding to six individuals, $n = 6$), growing near Balcarce, Buenos Aires province, Argentina. Asterisks indicate significant differences among races (Fisher's LSD test; $P < 0.05$).

	High wood density	Low wood density	Sig.
WBD (g cm^{-3})	0.65 ± 0.03	0.59 ± 0.04	*
Dh (μm)	49.94 ± 4.07	53.11 ± 6.60	
VN (mm^{-2})	78.08 ± 16.84	70.74 ± 19.14	
H (μm^2)	2090.41 ± 291.60	2513.59 ± 566.29	*
Rn (no. mm^{-1})	22.48 ± 3.05	24.17 ± 4.55	
FWT (μm)	1.855 ± 0.12	1.82 ± 0.15	
WF (%)	66.46 ± 7.15	60.38 ± 4.83	*
APp (%)	9.53 ± 2.04	10.46 ± 2.40	
FTp (%)	5.27 ± 1.18	6.54 ± 1.56	*
VTp (%)	8.11 ± 1.66	8.82 ± 1.48	
Fp (%)	77.09 ± 4.05	74.18 ± 4.26	
Fl (μm)	543.77 ± 28.38	581.72 ± 18.54	*
FTl (μm)	448.58 ± 25.09	469.39 ± 25.87	
VTl (μm)	365.11 ± 17.81	378.46 ± 27.44	
Vl (μm)	242.07 ± 20.25	230.51 ± 24.66	
b PDFV	4.97 ± 0.34	5.34 ± 0.74	
c PDFV	4.41 ± 0.81	4.95 ± 0.77	

WBD: wood basic density; Dh: vessel hydraulic diameter; VN: vessel density; H: halo area; Rn: rays per linear millimetre; FWT: fibre wall thickness; WF: fibre wall fraction; APp: axial parenchyma percentage; FTp: fibre-tracheid percentage; VTp: VT percentage; Fp: fibre percentage; Fl: fibre length; FTl: fibre-tracheid length; VTl: VT length; Vl: vessel element length; *b* PDFV: scale parameter of Weibull probability density function; *c* PDFV: shape parameter of Weibull probability density function.

Concerning the proportion of different cellular elements, differences were only observed in fibre-tracheid percentage. That would be, in turn, responsible for the differences found in the halo area, because this cellular element is one of its main components. Fibres differed in length but not in wall thickness, although fibre wall fraction was greater in the higher wood density race.

Vulnerability to cavitation

As expected from vessel characteristics, there were no significant differences in measured $k_{s\ max}$ between races (Table 3). However, while no significant differences were found in the P_{12}, P_{50} and P_{88} were more negative in the high wood density race, i.e., higher resistance to cavitation (Table 3). In addition, through contingency tables analysis we found differences in VC curves between races ($\chi^2 = 267.21$, $P < 0.001$). However, this did not translate into a steeper slope (see Figure S1 available as Supplementary Data at *Tree Physiology* Online for the vulnerability curves of both races).

Relationship among traits

Due to the high number of variables analysed, we decided to group the results according to the degree of functional relationship and the type of measurement performed.

Among the most important relationships found in this study is the highly positive relationship between the H and $k_{s\ max}$ (Table 4). Halo area (H) also showed a significant correlation with both Dh and VN, besides displaying a different sign. Maximum hydraulic specific conductivity ($k_{s\ max}$) was negatively associated with WBD and Rn and exhibited a positive relationship with the slope of VC curve. This last variable was correlated negatively with WBD (i.e., the lower the density, the steeper the slope) and positively with H and VTl. Due to the calculation method (one variable depending on the other), the slope was highly and positively correlated with P_{88}.

In addition to $k_{s\ max}$ and slope, WBD had a negative association with Dh, H, fibre-tracheid fraction and length and P_{88}, having only a positive correlation with WF.

The length of the accompanying fibrous cells (fibre, fibre-tracheids and vasicentric tracheids) was positively correlated with Dh and H (Table 4), suggesting structural relationships between the different cell types at both radial/transversal and longitudinal axes.

Path analysis

According to the PA (Figure 1), the main exogenous variables predicting vulnerability to cavitation are Dh and WF. Fibre wall fraction (WF) showed a direct impact on WBD (positive) and the slope of vulnerability curve (the greater the fibre wall fraction, the less steep the slope), and an indirect and negative effect over P_{50} through them. On the other hand, Dh exhibited a direct positive impact over $k_{s\ max}$ and negative over wood density (WBD). Wood basic density had a negative impact over P_{50} (i.e., the higher the wood density, the lower the vulnerability to cavitation), while this variable was positively correlated with the slope (the steeper the slope, the higher the P_{50} and vice versa). The slope of VC curve was directly and positively affected by $k_{s\ max}$. According to this model, Dh also showed a direct negative effect on P_{50}, i.e., the larger the vessels, the lower the VC, but an indirect and positive influence over this variable through WBD on one hand, and through $k_{s\ max}$ and slope on the other.

Almost all the goodness-of-fit tests carried out entered within the previously established range of acceptance. The only exception was the Normed Fit Index (NFI), which is not recommended for small samples since it could underestimate the fit of the model (Ullman 2013). Consequently, based on these results, we can conclude that the proposed model adequately fits the data (Table 5).

Discussion

The lack of correlation between wall thickness and wood basic density could be explained by the importance of cell lumen diameter (not measured) when defining fibre dimensions. Fibres constitute the cellular element in greatest proportion within xylem

Table 3. Mean ± standard deviation of hydraulic variables measured in two races of *Eucalyptus globulus* with high and low wood density respectively (12 curves for each race corresponding to six individuals), growing near Balcarce, Buenos Aires province, Argentina. Asterisks indicate significant differences among races (Fisher's LSD test; $P < 0.05$).

	High wood density	Low wood density	Sig.
$k_{s\ max}$ (kg m^{-1} $MPa^{-1}s^{-1}$)	1.55 ± 0.76	2.20 ± 1.46	
P_{12} (MPa)	−2.13 ± 1.02	−1.51 ± 0.78	
P_{50} (MPa)	−3.73 ± 1.27	−2.70 ± 1.02	*
P_{88} (MPa)	−5.62 ± 1.79	−4.10 ± 1.37	*
Slope of VC curve (%)	25.82 ± 10.74	35.36 ± 18.60	

and, therefore, their size (wall thickness + lumen diameter) has a great impact on wood density (Jacobsen et al. 2005). As a result, the relationship between these variables is often positive (Carrillo et al. 2015), negative (Martínez-Cabrera et al. 2009) or non-existent (Sterck et al. 2012, Barotto et al. 2016). On the other hand, fibre wall fraction (an indirect and relative measurement of wall thickness, which takes into account the fibre lumen) showed a highly significant and positive relationship with wood basic density, and it was the major predictor of this wood property. Since wood density reflects not only the proportion of wall within the xylem but also the fraction of lumens, the negative relationship observed between wood density and vessel hydraulic diameter was expected and is in agreement with previous works (Jacobsen et al. 2005).

As expected, based on the correlation coefficients, the main predictor of maximum hydraulic specific conductivity was vessel hydraulic diameter. This is in line with Hagen–Poiseuille law and has been widely reported in many works, including *Eucalyptus* species (e.g., Barotto et al. 2016). The relationship of $k_{s\ max}$ and the slope of VC curve was previously addressed by Barotto et al. (2016) working with three *Eucalyptus* species, including *E. globulus*. It suggests a trade-off between xylem efficiency and safety since the steeper the slope, the faster the development of cavitation process. Due to the positive correlation between this slope and P_{50} (path analysis), there is also an indirect trade-off between $k_{s\ max}$ and P_{50}. Also, a positive correlation was observed between the slope and P_{88}, indicating that the steeper the slope, the lower the cavitation resistance, at least at medium to low water potential values. Another relationship arose suggesting a positive effect of hydraulic diameter on P_{50} through wood density: an increase in Dh results in lower wood density, and this leads to higher P_{50}—higher vulnerability to cavitation. This trade-off between xylem efficiency and safety, though weak in this study (see next paragraph), has been shown in previous works at the interspecific level across woody plant species (Maherali et al. 2004, Gleason et al. 2016) or at the intraspecific level considering different size ranges of vessels (Cai and Tyree 2010).

In contrast to the sign of those indirect effects of Dh over P_{50}—through k_s and the slope of the VC curve and wood density—a direct and negative effect was observed. Therefore, it seems that the relationship between hydraulic diameter and vulnerability to cavitation is complex, with direct and indirect effects both positive and negative, resulting as a whole in a lack of compromise between hydraulic safety and efficiency. The direct relationship suggests that cavitation resistance does not escalate directly with vessel diameter, but depends on pit structure and size (Tyree and Sperry 1989) and/or the complex array of cells accompanying each vessel (the larger the vessel, the larger the halo area) which could act as a barrier for embolism spread (Cai et al. 2014). Similar results have been found in both gymnosperms (Burguess et al. 2006) and angiosperms (Vander Willigen et al. 2000), including an interspecific survey of three *Eucalyptus* temperate species (Barotto et al. 2016). This would suggest that the trade-off between conduction efficiency and safety has no evolutionary basis but depends more on species anatomy and the particular arrangement of the different cell types that compose it, within certain limits. In addition, we can hypothesize that vessel dimensions do not play a direct role in cavitation resistance, which seems to be an integrated measure that reflects the interaction of the different cell types involved in water transport through the xylem, interactions that may be directly or indirectly affected by cells dimensions and their spatial distribution.

On the other hand, despite the lack of correlation between fibre wall fraction and cavitation resistance, we found a mediated effect of the former anatomical trait on the functional one through wood basic density and slope. These results—which are in agreement with previous findings of Jacobsen et al. (2005) in shrubs species of arid environments—could suggest that the fibre matrix, in solitary vessel species like *Eucalyptus*, could contribute to mechanical support of vessels during water movement under high tension and/or act as a barrier for air passage between embolized and non-embolized vessels. This should affect the development of the cavitation event, being quantified through the slope of the vulnerability curve.

The P_{50} values obtained in this study are below those found for *E. globulus* by Pita et al. (2003) working with young cuttings, and Barotto et al. (2016) using branches of mature trees from non-commercial plantations. Working with adult trees from a genetic improvement programme may be partly responsible for the increased resistance, although this was not a target trait of the selection process. In our study, we found differences in vulnerability to cavitation between *E. globulus* races with different stem wood density. This was also manifested in the negative correlation between P_{88} and wood density, as well as in the path coefficient linking wood density with P_{50} in the model developed by path analysis. These findings at the intraspecific level are in agreement with a general trend at the interspecific level establishing an increase in cavitation resistance with wood density

Table 4. Correlation analysis among variables in two races of *Eucalyptus globulus* with high and low wood density, growing near Balcarce, Buenos Aires province, Argentina. * $P < 0.05$; ** $P < 0.01$; *** $P < 0.001$.

		Vessel related variables			Non-vessel related variables			Proportion of cellular elements				Length of cellular elements				Hydraulic measurements			
	WBD	Dh	VN	H	Rn	FWT	WF	Fp	APp	FTp	VTp	Fl	FTl	VTl	Vl	$k_{s\ max}$	P_{12}	P_{50}	P_{88}
Dh	−0.51**																		
VN		−0.59**																	
H	−0.45*	0.87***	−0.7***																
Rn		−0.48*		−0.45*															
FWT																			
WF	0.71***																		
Fp							0.41*												
APp								−0.9***											
FTp	−0.45*							−0.66***											
VTp								−0.83***	0.7***										
Fl	−0.51*	0.47*		0.52**			−0.42*												
FTl				0.44*								0.66***							
VTl		0.50*		0.52**									0.69***						
Vl										−0.53**				0.47*					
$k_{s\ max}$	−0.51*	0.83***	−0.54**	0.81***	−0.44*									0.46*					
P_{12}		−0.41*																	
P_{50}																	0.9***		
P_{88}	−0.46*						−0.42*										0.6**	0.89***	
slope	−0.52**			0.5*			−0.46*							0.41*		0.62**		0.42*	0.69***

Dh: vessel hydraulic diameter; VN: vessel density; H: halo area; Rn: rays per linear millimetre; FWT: fibre wall thickness; WF: fibre wall fraction; Fp: fibre percentage; APp: axial parenchyma percentage; FTp: fibre-tracheid percentage; VTp: VT percentage; Fl: fibre length; FTl: fibre-tracheid length; VTl: VT length; Vl: vessel element length; $k_{s\ max}$: maximum hydraulic specific conductivity; P_{12}: pressure inducing 12% loss of conductivity; P_{50}: pressure inducing 50% loss of hydraulic conductivity; P_{88}: pressure inducing 88% loss of hydraulic conductivity; slope: slope of vulnerability to cavitation curve; WBD: wood basic density.

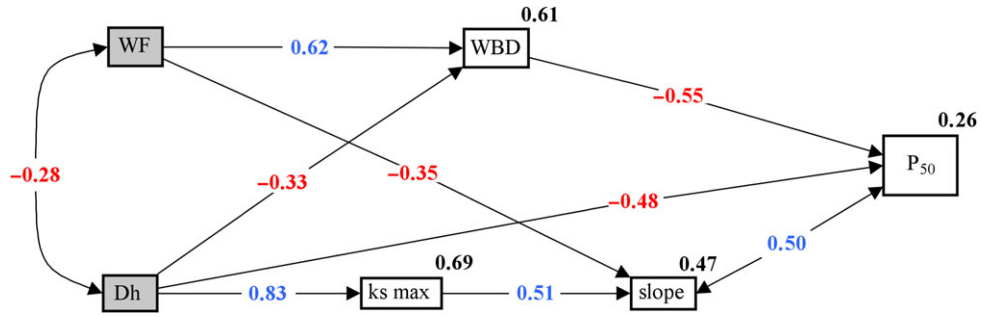

Figure 1. Final model developed by path analysis technique. The values in double-headed arrows correspond to Pearson correlation coefficient, values in straight single headed lines are the standardized path coefficients (*beta* weights in multiple regression) and values next to variables are the squared multiple correlations. Filled boxes represent exogenous variables, and open boxes represent endogenous variables. WF: fibre wall fraction; Dh: vessel hydraulic diameter; $k_{s\ max}$: maximum hydraulic specific conductivity; WBD: wood basic density; slope: slope of vulnerability to cavitation curve; P_{50}: pressure inducing 50% loss of hydraulic conductivity.

Table 5. Results of goodness-of-fit test for the proposed model.

Test	Value
χ^2	5.258; $P = 0.511$
χ^2/df	0.876
GFI	0.929
RMSEA	0
SRMR	0.054
NFI	0.939
TLI	1
CFI	1

(Hacke et al. 2001). However, it is interesting to point out that the potential cause of the relationship between wood density and resistance to cavitation observed by Hacke et al. (2001)—that is, the need to cell wall reinforcement to avoid cell collapse of a functional vessel (under tension) when it is in direct contact with an embolized one—cannot be applied to *Eucalyptus* species, or other species with solitary vessels, in which this imbalance of forces at both sides of the cell wall cannot be observed due to this peculiar vessel arrangement. Therefore, the relationship between wood density and resistance to cavitation in these species must be explained with other hypotheses, such as that proposed by Jacobsen et al. (2005) about the role of thick-walled fibres in the prevention of cavitation in adjacent vessels. Furthermore, this hypothesis sounds more likely—not only in species with solitary vessels—considering the quantitative contribution of fibre walls to explain wood density in angiosperm species (Ziemińska et al. 2013).

Conclusions

The results of this study, the first one to our knowledge studying the intraspecific variability of xylem cavitation in a *Eucalyptus* species and the influence of wood anatomy and density on it, suggest that variability in this trait is associated with wood density. Progenies with higher wood density at the stem level presented also higher wood density at the branch level, and they had higher resistance to cavitation. Moreover, in addition to the non-significant correlation between Dh and P_{50}, the path analysis suggests a lack of compromise between xylem efficiency and safety at the intraspecific level, the latter variable being the result of the combination of both positive and negative effects of vessel size. This complex relationship, which is also manifested by the small determination coefficient corresponding to P_{50}, seems to be a reflection of the intricate and particular wood anatomy present in this genus. There are no data about the relationship between growth and hydraulic efficiency in *E. globulus*, but we can hypothesize—based on results in other species showing a direct relationship between both traits—that, within this species, the trade-off between growth and xylem safety can also be avoided, and that wood density could be used as a proxy trait of this xylem function. However, more studies are needed to increase the number of genotypes in a broader wood density range and analyse the heritability of the studied traits, including not only wood density but also complementary traits, such as mean hydraulic diameter, since the effect of wood density over P_{50} is significant but quite low.

Supplementary Data

Supplementary Data for this article are available at *Tree Physiology* Online.

Acknowledgments

We thank Pablo Pathauer for providing us with information on wood density and for collaborating in the selection of races to be tested. The studies presented in this article have been developed in the framework of the international cooperation project 'TOPWOOD: Wood phenotyping tools: properties, functions and quality' (H2020-MSCA-RISE-2014 -European Commission).

Conflict of interest

None declared.

References

Barotto AJ, Fernandez ME, Gyenge J et al. (2016) First insights into the functional role of vasicentric tracheids and parenchyma in *Eucalyptus* species with solitary vessels: do they contribute to xylem efficiency or safety? Tree Physiol 36:1485–1497.

Burguess SSO, Pittermann J, Dawson TE (2006) Hydraulic efficiency and safety of branch xylem increases with height in *Sequoia sempervirens* (D. Don) crowns. Plant Cell Environ 29:229–239.

Cai J, Tyree MT (2010) The impact of vessel size on vulnerability curves: data and models for within-species variability in saplings of aspen, *Populus tremuloides* Michx. Plant Cell Environ 33:1059–1069.

Cai J, Li S, Zhang H et al. (2014) Recalcitrant vulnerability curves: methods of analysis and the concept of fibre bridges for enhanced cavitation resistance. Plant Cell Environ 37:35–44.

Carrillo I, Aguayo MG, Valenzuela S et al. (2015) Variations in wood anatomy and fiber biometry of *Eucalyptus globulus* genotypes with different wood density. Wood Res 60:1–10.

Cochard H, Badel E, Herbette S et al. (2013) Methods for measuring plant vulnerability to cavitation: a critical review. J Exp Bot 64:4779–4791.

Dai A (2013) Increasing drought under global warming in observations and models. Nat Clim Chang 3:52–58.

Dalla-Salda G, Martinez-Meier A, Cochard H et al. (2011) Genetic variation of xylem hydraulic properties shows that wood density is involved in adaptation to drought in Douglas-fir (*Pseudotsuga menziesii* (Mirb.)). Ann For Sci 68:747–757.

Dalla-Salda G, Fernández ME, Sergent AS et al. (2014) Dynamics of cavitation in a Douglas-fir tree-ring: transition-wood, the lord of the ring? J Plant Hydraul 1:e–0005.

Domec JC, Gartner BL (2001) Cavitation and water storage capacity in bole xylem segments of mature and young Douglas-fir trees. Trees Struct Funct 15:204–214.

Drew DM, O'Grady AP, Downes GM et al. (2008) Daily patterns of stem size variation in irrigated and unirrigated *Eucalyptus globulus*. Tree Physiol 28:1573–1581.

Drew DM, Downes GM, O'Grady AP et al. (2009) High resolution temporal variation in wood properties in irrigated and non-irrigated *Eucalyptus globulus*. Ann For Sci 66:406.

Franklin GL (1945) Preparation of thin sections of synthetic resins and wood-resin composites, and a new macerating method for wood. Nature 155:51.

Gleason SM, Westoby M, Jansen S et al. (2016) Weak tradeoff between xylem safety and xylem-specific hydraulic efficiency across the world's woody plant species. New Phytol 209:123–136.

Hacke UG, Sperry JS, Pockman WT et al. (2001) Trends in wood density and structure are linked to prevention of xylem implosion by negative pressure. Oecologia 126:457–461.

Hubbard RM, Ryan MG, Stiller V et al. (2001) Stomatal conductance and photosynthesis vary linearly with plant hydraulic conductance in *Ponderosa pine*. Plant Cell Environ 24:113–121.

InsideWood (2004–onwards) Published on the Internet. http://insidewood.lib.ncsu.edu/search (9 March 2017, date last accessed).

Jacobsen AL, Ewers FW, Pratt RB et al. (2005) Do xylem fibers affect vessel cavitation resistance? Plant Physiol 139:546–556.

Jacobsen AL, Agenbag L, Esler KJ et al. (2007) Xylem density, biomechanics and anatomical traits correlate with water stress in 17 evergreen shrub species of the Mediterranean-type climate region of South Africa. J Ecol 95:171–183.

Jinagool W, Rattanawong R, Sangsing K et al. (2015) Clonal variability for vulnerability to cavitation and other drought-related traits in *Hevea brasiliensis* Müll. Arg J Plant Hydraul 2:e001.

Lachenbruch B, McCulloh KA (2014) Traits, properties, and performance: how woody plants combine hydraulic and mechanical functions in a cell, tissue, or whole plant. New Phytol 204:747–764.

Lopez GA, Potts BM, Dutkowski GW et al. (2001) Quantitative genetics of *Eucalyptus globulus*: affinities of land race and native stand localities. Silvae Genet 50:244–252.

Maherali H, Pockman WT, Jackson RB (2004) Adaptive variation in the vulnerability of woody plants to xylem cavitation. Ecology 85:2184–2199.

Martínez-Cabrera HI, Jones CS, Espino S et al. (2009) Wood anatomy and wood density in shrubs: responses to varying aridity along transcontinental transects. Am J Bot 96:1388–1398.

Norman GR, Streiner DL (2003) Path analysis and structural equation modeling. In: Norman GR, Streiner DL (eds) PDQ statistics. BC Decker Inc., London, pp 156–176.

Pérez E, Medrano LA, Sánchez Rosas J (2013) El Path Analysis: conceptos básicos y ejemplos de aplicación. RACC 5:52–66.

Pita P, Gascó A, Pardos JA (2003) Xylem cavitation, leaf growth and leaf water potential in *Eucalyptus globulus* clones under well-watered and drought conditions. Funct Plant Biol 30:891–899.

Rosner S (2013) Hydraulic and biomechanical optimization in norway spruce trunkwood – a review. IAWA J 34:365–390.

Sparks JP, Black A (1999) Regulation of water loss in populations of *Populus trichocarpa*: the role of stomatal control in preventing xylem cavitation. Tree Physiol 19:453–459.

Sperry JS (1995) Limitations on stem water transport and their consequences. In: Gartner BL (ed) Plant stems: physiology and functional morphology. Academic Press, San Diego, CA, pp 105–124.

Sperry JS, Donnelly JR, Tyree MT (1988) A method for measuring hydraulic conductivity and embolism in xylem. Plant Cell Environ 11:35–40.

Sterck FJ, Martínez-Vilalta J, Mencuccini M et al. (2012) Understanding trait interactions and their impacts on growth in Scots pine branches across Europe. Funct Ecol 26:541–549.

Tesón N, Fernández ME, Licata J (2012) Resultados preliminares sobre la variación en vulnerabilidad a la cavitación por sequía en clones de Eucalyptus grandis. Congreso IUFRO 2012: "Eucaliptos mejorados para aumentar la competitividad del sector forestal en América Latina". November 22–23. Pucón, Chile.

Tyree MT, Sperry JS (1989) Vulnerability of xylem to cavitation and embolism. Annu Rev Plant Physiol Mol Biol 40:19–38.

Ullman JB (2013) Structural equation modeling. In: Tabachnick BG, Fidell LS (eds) Using multivariate statistics. Pearson Education, Inc., Boston, NJ, pp 681–785.

Vander Willigen C, Pammenter NW (1998) Relationship between growth and xylem hydraulic characteristics of clones of *Eucalyptus* spp. at contrasting sites. Tree Physiol 18:595–600.

Vander Willigen C, Sherwin HW, Pammenter NW (2000) Xylem hydraulic characteristics of subtropical trees from contrasting habitats grown under identical environmental conditions. New Phytol 145:51–59.

Ziemińska K, Butler DW, Gleason SM et al. (2013) Fibre wall and lumen fractions drive wood density variation across 24 Australian angiosperms. AoB Plants 5:plt046.